

## Supporting Information

### Influence of Chemical Composition on Proton Conductivity of Microporous Organic Polymers Entrapped in Nitrilotrimethylphosphonic Acid

Jiarui Du<sup>a</sup>, Feng Zhang<sup>a\*</sup>, Xiaoqiang Liang<sup>b\*</sup>, and Fengyu Qu<sup>a\*</sup>

*a. Key Laboratory of Photochemical Biomaterials and Energy Storage Materials,  
Heilongjiang Province and College of Chemistry and Chemical Engineering, Harbin  
Normal University, Harbin 150025, P. R. China*

*b. College of Environmental and Chemical Engineering, Xi'an Polytechnic  
University, Xi'an 710048, P. R. China*

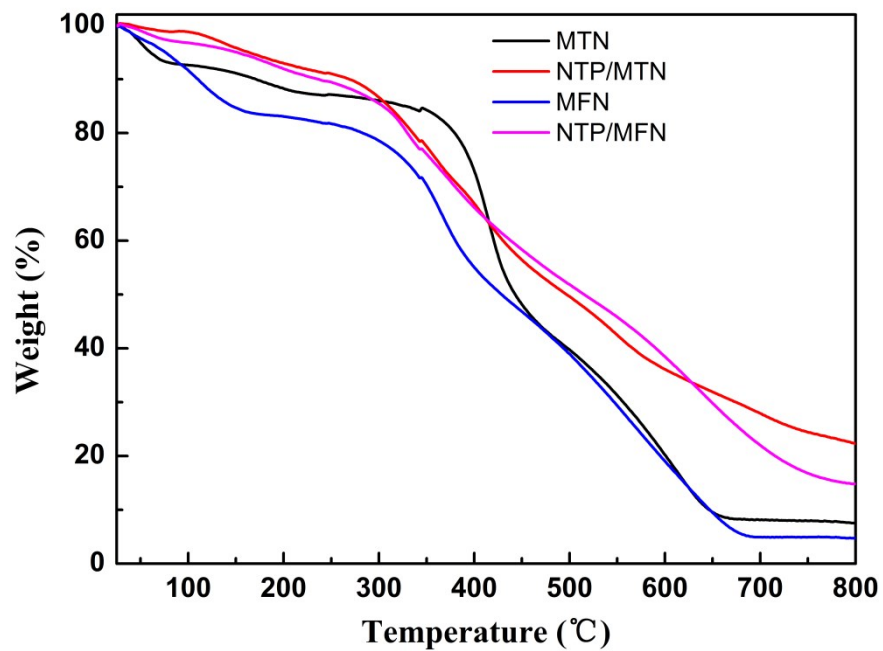


**Fig. S1** TGA curves of MTN, MFN, NTP/MTN and NTP/MFN.

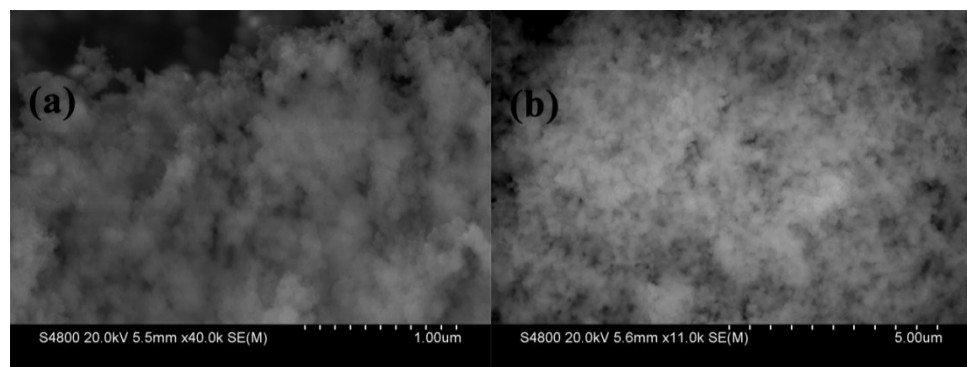


**Fig. S2** SEM images of (a) MTN and (b) NTP/MTN.

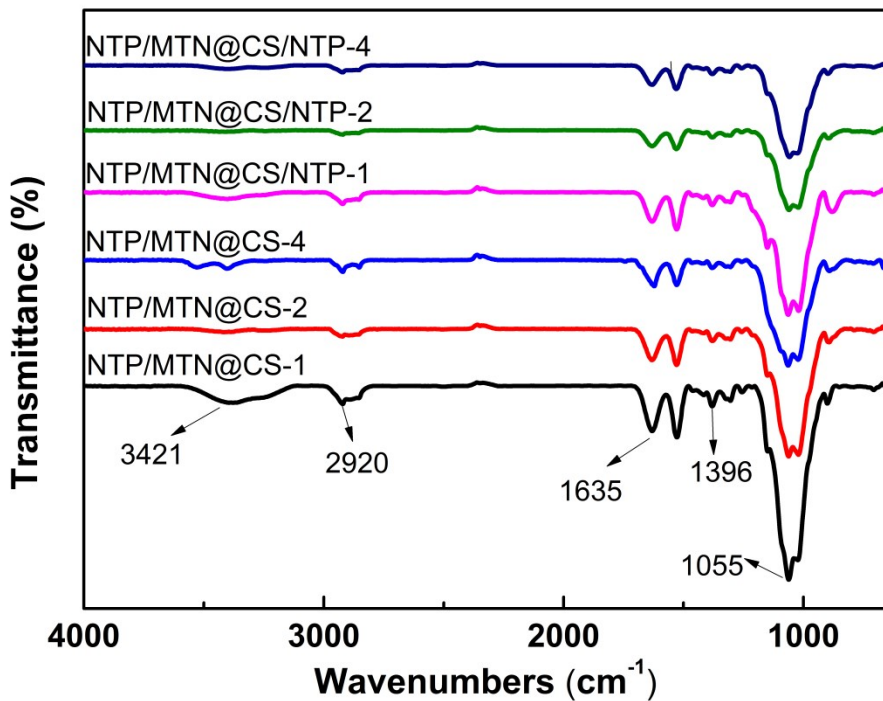


**Fig. S3** FT-IR spectra of NTP/MTN membranes.

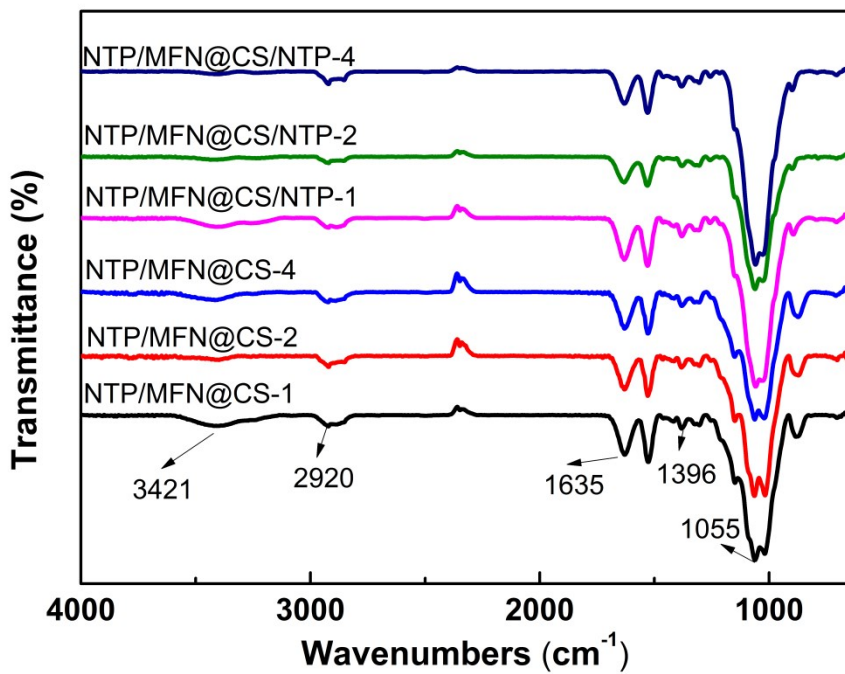


**Fig. S4** FT-IR spectra of NTP/MFN membranes.

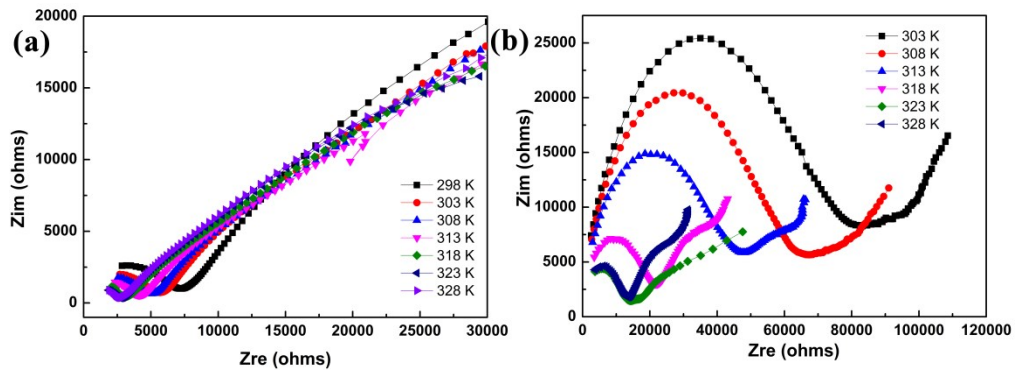


**Fig. S5** Nyquist plots of CS membranes at (a) ~98% RH and (b) ~76% RH.

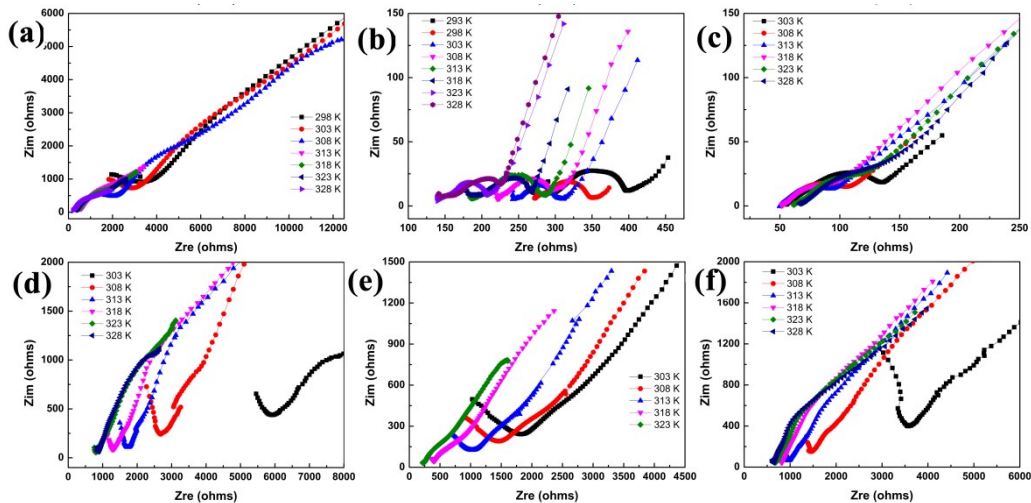


**Fig. S6** Nyquist plots of (a) NTP/MFN@CS-1, (b) NTP/MFN@CS-2 and (c) NTP/MFN@CS-4 (d) NTP/MFN@CS/NTP-1, (e) NTP/MFN@CS/NTP-2 and (f) NTP/MFN@CS/NTP-4 at ~98% RH.

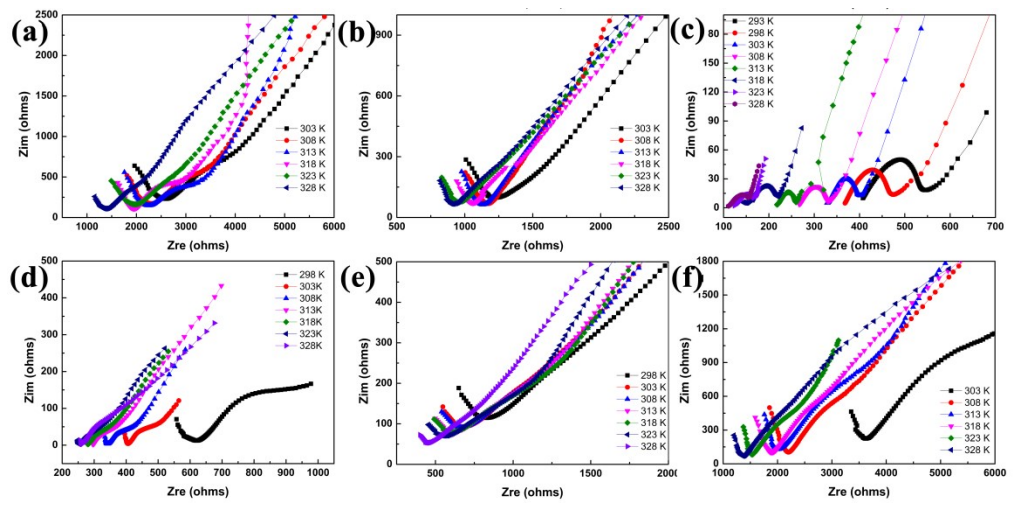


**Fig. S7** Nyquist plots of (a) NTP/MTN@CS-1, (b) NTP/MTN@CS-2 and (c) NTP/MTN@CS-4 (d) NTP/MTN@CS/NTP-1, (e) NTP/MTN@CS/NTP-2 and (f) NTP/MTN@CS/NTP-4 at ~98% RH.

---

**Table S1** CHN elemental analysis and ICP of MTN, NTP/MTN, MFN and NTP/MFN.

Samples	C (%)	H (%)	N (%)	S (%)	P (%)
MFN	33.83	4.78	46.13	0	0.0003
NTP/MFN	28.67	4.74	33.83	0	0.085
MTN	45.12	3.33	30.14	4.13	0.0002
NTP/MTN	32.44	3.35	23.62	3.01	0.083

---

**Table S2** Porosity parameters of MTN, NTP/MTN, MFN and NTP/MFN.

Samples	$S_{BET}$ ( $\text{cm}^2 \text{ g}^{-1}$ )	Pore volume ( $\text{cm}^3 \text{ g}^{-1}$ )
MFN	230.07	0.38
NTP/MFN	42.33	0.11
MTN	785.09	1.13
NTP/MTN	185.07	0.69

---

**Table S3** Ionic-exchange capability (IEC) and activation energy ( $E_a$ ) of membranes.

Sample	IEC (meq g <sup>-1</sup> )	$E_a$ (eV)	$\sigma$ (S cm <sup>-1</sup> )
MFN	0.15	/	/
NTP/MFN	6.58	/	/
MTN	0.045	/	/
NTP/MTN	5.78	/	/
NTP/MFN@CS-1	3.20	0.88	$1.9 \times 10^{-2}$
NTP/MFN@CS-2	4.40	0.83	$4.6 \times 10^{-2}$
NTP/MFN@CS-4	3.14	0.20	$5.5 \times 10^{-3}$
NTP/MFN@CS/NTP-1	0.53	0.70	$9.1 \times 10^{-4}$
NTP/MFN@CS/NTP-2	0.25	0.98	$3.4 \times 10^{-3}$
NTP/MFN@CS/NTP-4	0.32	0.58	$5.3 \times 10^{-4}$
NTP/MTN@CS-1	1.19	0.21	$1.1 \times 10^{-3}$
NTP/MTN@CS-2	1.25	0.14	$1.3 \times 10^{-3}$
NTP/MTN@CS-4	0.95	0.35	$3.4 \times 10^{-3}$
NTP/MTN@CS/NTP-1	1.19	0.21	$9.2 \times 10^{-3}$
NTP/MTN@CS/NTP-2	0.56	0.18	$1.1 \times 10^{-3}$
NTP/MTN@CS/NTP-4	0.34	0.48	$3.8 \times 10^{-4}$
CS	0.20	0.32	$1.1 \times 10^{-4}$

**Table S4** Proton conductivity of COF and membranes under ambient conditions.

Materials	Condition	$\sigma/\text{S cm}^{-1}$	Reference
I	55 °C, 99% RH	$6.17 \times 10^{-2}$	[1]
SZrTi	90°C, 100% RH	$2.9 \times 10^{-3}$	[2]
Fe-NH <sub>3</sub> -72h	80 °C, 95% RH	$1.8 \times 10^{-3}$	[3]
c-PBI-30	200 °C, 100% RH	$2.53 \times 10^{-1}$	[4]
FJU-80	80 °C, 98% RH	$1.05 \times 10^{-4}$	[5]
COF-1-Li	40 °C, 98% RH	$2.7 \times 10^{-2}$	[6]
COF-1-Na	40 °C, 98% RH	$2.5 \times 10^{-2}$	[6]
NH <sub>4</sub> PO <sub>3</sub> /MO <sub>2</sub>	175 °C, 99% RH	$8.5 \times 10^{-3}$	[7]
BaCe <sub>(0.85-x)</sub> Co <sub>x</sub> Gd <sub>0.15</sub> O <sub>3-δ</sub>	200 °C, 99% RH	$4.81 \times 10^{-3}$	[8]
Nafion/BP3-1.0	50 °C, 80% RH	$8.5 \times 10^{-2}$	[9]
SPS/POM-BC-30	25 °C, 100% RH	$5.3 \times 10^{-2}$	[10]
FJU-106	70 °C, 99% RH	$1.8 \times 10^{-2}$	[11]
h-BN	55 °C, 99% RH	$6.17 \times 10^{-2}$	[12]
Am3-sNCC-5	40 °C, 100% RH	$4.3 \times 10^{-2}$	[13]
NUS-10(R)@PVDF-50	25 °C, 100% RH	$5.16 \times 10^{-3}$	[14]
NTP/MFN@CS-2	50 °C, 98% RH	$4.6 \times 10^{-2}$	This work

## Reference

- [1] S. Thammakan, P. Rodlamul, N. Semakul, N. Yoshinari, A. Rujiwatra, *Inorg. Chem.*, 2020, **6**(59), 3518–3522.
- [2] S. Sarirchi, S. Rowshanzamir, F. Mehri, *Int. J. Energy Res.*, 2020, **44**(4) 2783–2800.
- [3] I.R. Salcedo, M. García, A. Cuesta, E.R. Losilla, A. Díaz, *Dalton Trans.*, 2020, **49**, 3981–3988.
- [4] X. Li, H. Ma, P. Wang, Z. Liu, M.D. Guiver, *Chem. Mater.*, 2020, **3**(32), 1182–1191.
- [5] Z. Que, Y. Ye, Y. Yang, F. Xiang, Z. Zhang, *Inorg. Chem.*, 2020, **5**(59),

---

3053–3061.

- [6] B. Zhou, J. B. Le, Z. Cheng, X. Zhao, H. Chen, *ACS Appl. Mater. Interfaces*, 2020, **12**(7), 8198-8205.
- [7] C. Sun, U. Stimming, *Electrochim. Acta*, 2008, **53**, 6417-6422.
- [8] G. Accardo, D. Frattini, S.P. Yoon, *J. Alloys Compd*, 2020, **834**, 155114.
- [9] F.C. Teixeira, A.I.d. Sá, A.P.S. Teixeira, V.M. Ortiz-Martínez, C.M. Rangel, *Int. J. Hydrogen Energy*, 2020, **45**(31) 15495-15506.
- [10] Y. Yin, H. Li, H. Wu, W. Wang, Z. Jiang, *Int. J. Hydrogen Energy*, 2020, **232**, 58-67.
- [11] Q. Lin, Y. Ye, L. Liu, Z. Yao, Z. Li, L. Wang, C. Liu, Z. Zhang, S. Xiang, *Nano Res.*, 2020, **14**, 387–391.
- [12] S.I. Yoon, K.Y. Ma, T.Y. Kim, H.S. Shin, *J. Mater. Chem.*, 2020, **8**, 2898-2912.
- [13] Q. Zhao, Y. Wei, C. Ni, L. Wang, *Appl. Surf. Sci.*, 2019, **466**, 691-702.
- [14] Y. Peng, G. Xu, Z. Hu, Y. Cheng, C. Chi, D. Yuan, H. Cheng and D. Zhao, *ACS Appl. Mater. Interfaces*, 2016, **8**, 18505-18512.